

Review

# The inorganic biochemistry of photosynthetic oxygen evolution/water oxidation

G.M. Ananyev<sup>1</sup>, L. Zaltsman, C. Vasko, G.C. Dismukes<sup>\*</sup>

*Princeton University Department of Chemistry, Hoyt Laboratory, Princeton, NJ 08544, USA*

Received 24 May 2000; received in revised form 29 August 2000; accepted 13 September 2000

## Abstract

At the request of the organizer of this special edition, we have attempted to do several things in this manuscript: (1) we present a mini-review of recent, selected, works on the light-induced inorganic biogenesis (photoactivation), composition and structure of the inorganic core responsible for photosynthetic water oxidation; (2) we summarize a new proposal for the evolutionary origin of the water oxidation catalyst which postulates a key role for bicarbonate in formation of the inorganic core; (3) we summarize published studies and present new results on what has been learned from studies of ‘inorganic mutants’ in which the endogenous cofactors ( $\text{Mn}^{n+}$ ,  $\text{Ca}^{2+}$ ,  $\text{Cl}^-$ ) are substituted; (4) the first  $\Delta\text{pH}$  changes measured during the photoactivation process are reported and used to develop a model for the stepwise photo-assembly process; (5) a comparative analysis is given of data in the literature on the kinetics of substrate water exchange and peroxide binding/dismutation which support a mechanistic model for water oxidation in general; (6) we discuss alternative interpretations of data in the literature with a view to forecast new avenues where progress is needed. © 2001 Elsevier Science B.V. All rights reserved.

## 1. Evolutionary origin of photosynthetic water oxidation

A major breakthrough in the evolution of life on earth was the creation of oxygen-producing organisms that used water as a reductant for photosynthesis. This event is estimated to have taken place circa 2.7–3.5 billion years ago and is believed to be responsible for conversion of our atmosphere from anaerobic to its present molecular oxygen ( $\text{O}_2$ ) rich composition [1]. The availability of  $\text{O}_2$  in the bio-

sphere enabled a second major breakthrough in evolution to occur, the creation of aerobic metabolism, which produces 18 times greater energy (ATP) per unit of substrate (glucose) than anaerobic metabolism. This event led to the evolution of complex organisms, including mammals.

How did the first oxygenic photosynthetic organism ‘learn’ to oxidize water instead of reduced carbon or sulfur compounds employed by all of its bacterial precursors?  $\text{O}_2$  production by water oxidation is the most energetically demanding biological redox reaction, in addition to requiring a complex five-step mechanism for removal of four electrons and four protons (S-state transitions). Evolutionary precursors (transitional organisms), which perform water oxidation/oxygen evolution by alternative chemistry than contemporary organisms, have not been identified to

<sup>\*</sup> Corresponding author. Fax: +1-609-258-1980; E-mail: [dismukes@princeton.edu](mailto:dismukes@princeton.edu)

<sup>1</sup> Present address: Rutgers University, Institute of Marine and Coastal Sciences, 71 Dudley Rd., New Brunswick, NJ 08901, USA.

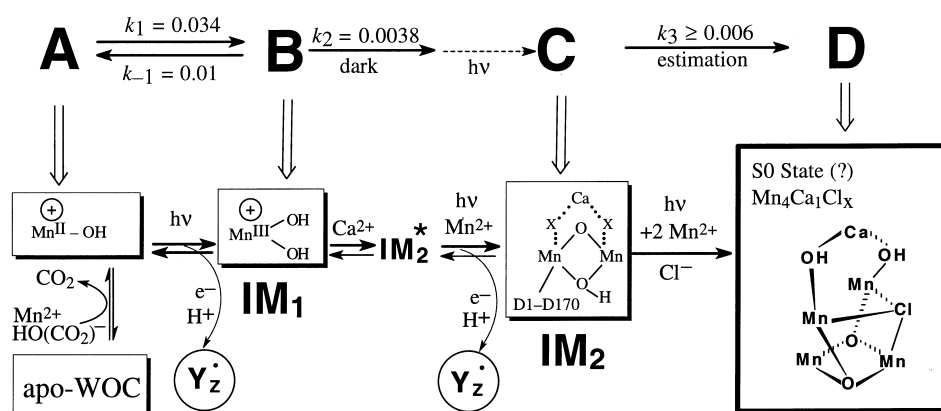
date. Two evolutionary processes had to occur. The creation of a stronger photo-oxidant than bacteriochlorophyll-a (BChl-a) in the reaction center, and the formation of a catalyst to enable concerted multi-electron oxidized intermediates to form.

BChl-a (0.55 V) was quite sufficient for the one-electron oxidation of reduced carbon and sulfur compounds utilized by non-oxygenic bacteria. A plausible case has been made for chlorophyll (Chl) pigment evolution from the moderate potential of BChl-a to the much stronger oxidant Chl-a (ca. 1.1 V) found in oxygenic organisms. This is hypothesized to have occurred via transitional organisms that first employed Chl-d [2]. Pigment evolution alone, however, cannot account for water oxidation, as the one-electron potential for the oxidation of water is much too high at 2.75 V. Hence, the acquisition of a catalyst is essential to access lower potential oxidation processes, either two-electron or four-electron concerted oxidation of water to  $\text{H}_2\text{O}_2$  (1.35 V) or  $\text{O}_2$  (0.82 V), respectively. So what was the chemical composition and structure of the first multi-electron catalyst and was there a transitional electron donor before water was adopted? Blankenship and Hartman have suggested that hydrogen peroxide may have been the transitional electron donor and that manganese could have been incorporated into photosystem (PS) II upon uptake of a dimanganese catalase enzyme via fusion with a non-photosynthetic bacterial precursor [2]. However, the first part of this hypothesis requires an abundant environmental source for hydrogen peroxide, which is not known to have existed under the mildly reducing conditions of the archaean period. The second hypothesis would suggest the existence of sequence homology between the catalase enzyme(s) and the manganese binding domain of the PSII D1 or D2 subunits. However, the recently available catalase sequence data appear not to support a similarity with PSII [3,4].

Baranov et al. have presented an alternative hypothesis based on the biogeochemical cycle of carbon dioxide and its hydrolysis products in water [5]. In their view, bicarbonate ion ( $\text{HCO}_3^-$ ) could have had a dominant role in altering the speciation of metal ions, particularly, manganese and calcium, in the archaean oceans owing to the enormously greater concentration of bicarbonate in equilibrium with atmospheric  $\text{CO}_2$  about 3–4 billion years ago ( $\text{CO}_2$

$10^2$ – $10^4$  above current partial pressure). They argue based on binding constant data that  $\text{Mn}(\text{HCO}_3)^+$  and  $[\text{Mn}(\text{HCO}_3)_2]_n$  complexes would have existed as the major aqueous forms under archaean conditions ( $[\text{Mn}] = 0.002$  ppm in seawater today) [6]. Recent unpublished EPR and electrochemical work has also found evidence for formation of  $\text{Mn}_X$  clusters specifically in the presence of bicarbonate ( $> 0.1$  M) (Kozlov, Y.N., Klimov, V.V., Tyrshkin, A., Dasgupta, J. and Dismukes, G.C., unpublished). Further, since these species are considerably easier to oxidize than aquo  $\text{Mn}^{2+}$  (1.2–1.4 V) at  $\sim 0.92$  V and 0.63 V, respectively, they could have been bound and photo-oxidized even by purple bacterial reaction centers to form the initial precursor to the inorganic core of the water oxidizing complex (WOC). Baranov et al. [5] presented evidence to support this hypothesis from photoactivation studies of apo-WOC-PSII in contemporary organisms such as spinach and wheat. Low levels of bicarbonate ( $< 25$   $\mu\text{M}$ ) were shown to accelerate the binding and photo-oxidation of  $\text{Mn}^{2+}$  in the first step of photoactivation by increasing the binding affinity of the first  $\text{Mn}^{2+}$ . Several compatible models were discussed to account for the data, including the possibility that bicarbonate delivers hydroxide needed for binding of  $\text{Mn}(\text{OH})^+$  to apo-WOC and for oxidation to  $\text{Mn}(\text{OH})^{2+}$  in the first photolytic step of photoactivation (Scheme 1).

Calcium is known to competitively inhibit the binding of  $\text{Mn}^{2+}$  at the high-affinity site during photoactivation [7]. Interestingly, bicarbonate was found to stimulate photoactivation at a second site by complexation of free  $\text{Ca}^{2+}$ , thereby reducing its activity in competing with  $\text{Mn}^{2+}$  in the formation of the first photoactivation intermediate ( $\text{IM}_1$ , Scheme 1) [5]. The complexation of free  $\text{Ca}^{2+}$  by bicarbonate in the photoactivation solution ( $K_D \sim 5$ – $10$  mM range) had no effect on the rate of uptake of calcium at its effector site – the site involving the dark step of photoactivation ( $\text{Ca}^{2+}$  binding to  $\text{IM}_1$ , Scheme 1) and for restoration of  $\text{O}_2$  evolution. Thus, at the concentrations of bicarbonate (2 mM) and calcium (400 ppm) found in the contemporary ocean, one can expect both sites for bicarbonate action to contribute importantly to acceleration of the photoactivation process. On this basis, one can imagine that bicarbonate may have been adopted to suppress photo-inactivation within marine cyanobacteria that are ex-



Scheme 1. The sequence of kinetic intermediates formed during assembly of the inorganic core of the WOC by photoactivation, including a role for bicarbonate. The pseudo-first-order rate constants are in units of  $\text{s}^{-1}$  and, in the case of  $k_1$ ,  $k_{-1}$  and  $k_2$ , refer to the initial conditions described by Zaltsman et al. [7] with concentrations  $[\text{Ca}] = 8 \text{ mM}$ ,  $[\text{Mn}] = 8 \text{ }\mu\text{M}$ ,  $[\text{apo-WOC-PSII}] = 1 \text{ }\mu\text{M}$  and  $\text{pH} = 6.5$ . The rate constant  $k_3$  was estimated by numerical modeling as described in the text. The structural model for the terminal photoactivated state ( $\text{S}_0$  state) is not based on photoactivation data.

posed to both high levels of calcium and high solar irradiance in the tropics.

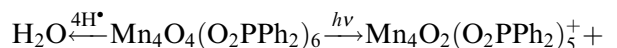
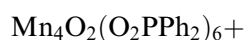
The prediction that  $[\text{Mn}(\text{HCO}_3)_2]_n$  clusters could have existed in the archaean oceans as a major form of dissolved manganese leads to another important condition for the evolution of aerobic life forms, including oxygenic photosynthesis. Namely, the presence of an abiotic catalase system for the efficient dismutation of hydrogen peroxide that would surely have formed by reduction of dissolved  $\text{O}_2$  under the mildly reducing environment predicted to have existed in the archaean period [8].  $[\text{Mn}(\text{HCO}_3)_2]_n$  clusters are known to be efficient non-enzymatic catalases that are orders of magnitude more reactive than the corresponding concentration of free  $\text{Mn}^{2+}$  [9]. Hydrogen peroxide is a potent antibiotic owing to its much higher reactivity than oxygen in generation of free radicals. Therefore, the  $[\text{Mn}(\text{HCO}_3)_2]_n$  clusters in the environment would have protected all organisms, including the first  $\text{O}_2$ -evolving organisms from destructive oxidation from peroxide prior to the evolution of an enzymatic catalase system.

There is a long and rich history concerning the role of bicarbonate in PSII function (see Baranov et al. [5] for a listing of some earlier works). Metzner, Govindjee and Stemler first suggested a possible site for bicarbonate on the donor side of PSII, which was later refuted by Radmer and Ollinger based on isotopic studies. The subsequent discovery of strong evidence for a bicarbonate binding site associated

with the non-heme iron on the acceptor side in PSII shifted the attention of most researchers away from the earlier hypothesis. More recently, Klimov's group and their collaborators followed up on these earlier works and found compelling evidence showing the involvement of bicarbonate in promoting electron donation from free  $\text{Mn}^{2+}$  to apo-WOC-PSII, and also for enhancing light-induced charge separation within holo-WOC-PSII [10–14]. Baranov et al. provided the missing evidence linking bicarbonate to assembly of the inorganic core required for  $\text{O}_2$  evolution. The Pushchino group has proposed a direct role for bicarbonate as an intrinsic cofactor within the WOC [12]. Direct spectroscopic evidence identifying the location and characteristics of the binding site for bicarbonate in the WOC (rather than alternatively delivering  $\text{OH}^-$ ) is still lacking. Further work in progress may clarify this picture.

Additional evidence in support of a special role for bicarbonate in assembly of the tetra-manganese core of the WOC comes from synthetic modeling studies. It has been found that simple phosphinate anions ( $\text{RRPO}_2^-$ ), which function much like non-hydrolyzable iso-structural 'bicarbonate surrogates', induce spontaneous assembly of tetra-manganese-oxo clusters,  $\text{Mn}_4\text{O}_4(\text{O}_2\text{PPh}_2)_6$  [15,16], having a cubane core structure analogous to our conjectural proposal for the  $\text{S}_4$ -WOC core. Significantly, the cubanes have been found to functionally mimic the overall process of water oxidation and  $\text{O}_2$  evolution by undergoing

both  $4e^-/4H^+$  reductive dehydration and photochemically triggered release of  $O_2$ , Eq. 1 [17,18]



## 2. Assembly of the inorganic core of the WOC by photoactivation

According to present knowledge, all species so far investigated that produce oxygen by photosynthesis utilize the same inorganic core for catalysis. Independent evidence from several sources indicates a stoichiometry of four manganese ions (reviewed in [19,20]), one calcium ion [21,22] and as few as one chloride ion [23,24] are needed for activity. Oxygen atoms in the form of oxide, hydroxide and/or water molecules are also associated with the WOC in an unknown stoichiometry and may originate from solvent and possibly bicarbonate. The manganese cluster is the redox-active site for charge accumulation and is known to bind a small number of water molecules that are exchangeable with bulk water based on ENDOR, ESEEM and nuclear magnetic resonance (NMR) studies (see for example [25,26] and Section 3). These inorganic cofactors along with the redox-active tyrosine-Z ( $Y_Z$ ) and other critical residues in the D1 subunit comprise what is called the WOC of PSII (WOC-PSII) or oxygen-evolving complex (OEC).

During biogenesis of the PSII-WOC complex, the component proteins are synthesized and inserted into the thylakoid membrane. The free inorganic cofactors are subsequently taken up from the luminal space under the control of light to form a functional WOC capable of stable  $O_2$  production from water. Chenaie and coworkers coined the phrase photoactivation to denote this process and demonstrated it to be a two-step light-driven process. In the past 30 years, many studies have provided insights into the photoactivation process, particularly the pioneering work by Chenaie and his coworkers. These works include: (1) the role of  $Mn^{2+}$ ,  $Ca^{2+}$ ,  $Cl^-$  and the experimental conditions (light intensity, pH, type of

buffer and exogenous electron acceptor, method for removal of Mn) [27–34]; (2) identification of essential amino acid residues for assembly and possible Mn ligands [35–41]; (3) the time-course for recovery of  $O_2$  evolution under continuous and intermittent light has led to a widely accepted kinetic model for assembly of the cluster, involving sequential light and dark steps of Mn ligation and photo-oxidation leading to formation of the tetra-Mn cluster [37,42,43]; (4) a model for reassembly of the extrinsic polypeptides of PSII and their role in enhancing the affinity or stability of one or more of the inorganic cofactors [44–48].

### 2.1. Proteins

No chaperone proteins have been found to be essential for photoactivation, although conformational roles for non-liganding domains of the PSII core appear to be important [49,50]. Büchel et al. showed that the minimal protein core that is needed for photoactivation is comprised of the four PSII reaction center subunits (D1, D2, Cyt *b*-559 ( $\alpha+\beta$  subunits)), an inner antenna subunit CP47 and several smaller hydrophobic subunits [51]. The additional inner antenna core subunit CP43, which together with the other subunits makes up what had traditionally been thought to be the minimal PSII core, was found not required for photoactivation. However, its presence in the core increases the rate of photoactivation by stabilizing the light-induced intermediates from decay and increases the cross section for light absorption. The quantum efficiency for photoactivation at limiting light flux was found to increase in direct proportion to the size of the Chl antenna size (CP47RC < PSII core < PSII/LHC).

In higher plants, three extrinsic proteins cap the PSII core polypeptides and play important roles in the long-term stability against reductants (diffusional barrier) and in the affinities for chloride and calcium [19,52,53]. However, they are not essential for photoactivation *in vitro*. The 33 kDa extrinsic protein (MSP-33), present in all oxygenic cyanobacteria and higher plants, when removed lowers the  $O_2$  activity to ca. 35% under steady-state turnover. This appears to result from a thermodynamic stabilization of the  $S_2$  and  $S_3$  states and kinetic retardation of the  $O_2$ -evolving step ( $S_4 \rightarrow S_0$ ). Studies of deletion mu-

tants show that the presence of the MSP-33 in algal cells actually retards the kinetics of assembly by serving as a diffusional barrier against  $\text{Mn}^{2+}$  binding, but is critical for long-term stability of the WOC [46,54].

In vivo photoactivation studies in the deletion mutant (FUD 39) of the green alga *Chlamydomonas reinhardtii* which lacks the psbP gene encoding the 23 kDa extrinsic protein has shown that this protein plays a role in suppressing photoinactivation in high light intensity [55]. Considering earlier data, this result probably indicates the role of the 23 kDa subunit in enhancing the affinity of the inorganic cofactors, particularly chloride and calcium [19,52]. Similar studies of in vivo photoactivation have indicated an electron donor role for  $\text{Y}_D$  and Cyt *b*-559 in reducing the effects of photoinactivation prior to assembly of the functional WOC cluster [56].

## 2.2. Manganese

Kinetic resolution of the photoactivation process has enabled identification of the cofactor requirements in each of the first two steps. Previous estimates indicate that 3–5  $\text{Mn}^{2+}$  ions bind to the apo-WOC-PSII protein complex during photoactivation [42] or four  $\text{Mn}^{2+}$  per PSII RC at sites that interact cooperatively [20]. One manganese ion binds first in the dark to a high-affinity site whose affinity is tuned to recognize  $\text{Mn}(\text{OH})^+$  specifically over  $\text{Mn}^{2+}$ .

A compelling kinetic proof showing that a stoichiometry of exactly 4.0  $\text{Mn}/\text{PSII}$  is needed for photoactivation is shown in Fig. 1. This figure presents a titration, as a function of the added  $\text{Mn}^{2+}$  concentration, of the transit time for formation of the first intermediate  $\text{IM}_1$  from apo-WOC-PSII ( $\tau$ -lag). Since only PSII centers that produce  $\text{O}_2$  are detected, the  $X$ -intercept should indicate the amount of  $\text{Mn}/\text{PSII}$  required to ‘turn on’ the detector, while the slope gives the molecularity required to advance to  $\text{IM}_1$ . One can see that the initial slope (I) is first-order in  $\text{Mn}^{2+}$ , while the  $X$ -intercept (I-II) gives a stoichiometry of 4.0  $\text{Mn}/\text{PSII}$  for  $\text{O}_2$  production, after removal of the weak interference (slope II) arising from the effect of excess  $\text{Mn}^{2+}$ . What is significant about this kinetic approach is that in principle the sample could be loaded with lots of other centers or ligands that bind  $\text{Mn}^{2+}$ , but otherwise does not interfere with the kinetic determination of the amount of Mn required

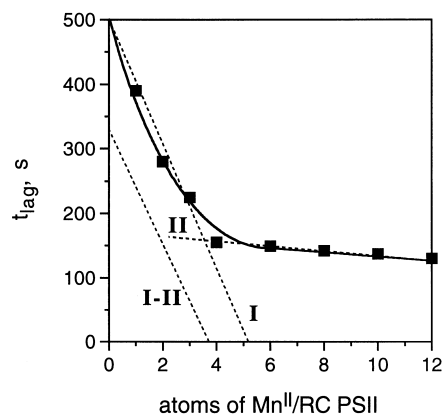


Fig. 1. Titration of the photoactivation lag-time as a function of the concentration of added  $\text{Mn}^{2+}$  (in units of PSII stoichiometry). Assay conditions [7]: apo-WOC-PSII membranes at 0.25 mg of Chl, 25 mM MES-NaCl buffer (pH 6.0), 35 mM NaCl, 300 mM sucrose, 0.8 mM ferricyanide. PSII membranes were extracted with chelator TPDBA. Photoactivation conditions: duration of light pulse 40 ms, dark time 2 s, total time of pulse-light photoactivation 15 min, light intensity 80 mW/cm<sup>2</sup>.

for photoactivation. The same is not true of data based on the yield of active centers. The kinetic method requires complete removal of labile Mn from the WOC, which is possible via proper use of chelators or reducing agents plus  $\text{MgCl}_2$  [57].

The pH dependence of photoactivation is consistent with the release of protons or equivalently the uptake of hydroxide in the initial steps of assembly [20]. This selection of the singly charged  $\text{Mn}(\text{OH})^+$  complex is seen also in the inhibition by both divalent and monovalent metal cations and oxo-metal cations (vanadyl,  $\text{VO}^{2+}$  and uranyl,  $\text{OUO}^{2+}$ ) [58]. Binding to this site is strongest for divalent ions that have the highest binding constant for hydroxide ( $\text{Zn}^{2+} > \text{Mn}^{2+} \gg \text{Ca}^{2+}$ ). Inhibition at this site by the alkali metal ions follows the reverse sequence ( $\text{Cs}^+ > \text{Rb}^+ > \text{K}^+ > \text{Na}^+ > \text{Li}^+$ ) with the larger size ions binding more strongly and surprisingly slightly stronger binding by  $\text{Cs}^+$  than  $\text{Mn}(\text{OH})^+$  (at pH 6.0). The alkali ions do not undergo hydrolysis and so bind as the mono-charged ions, hence the reason for the greater affinity for  $\text{Cs}^+$  which is closest in size to  $\text{Mn}(\text{OH})^+$ . Because addition of  $\text{HCO}_3^-$  accelerates the uptake of the first  $\text{Mn}^{2+}$ , the current model we favor employs  $\text{HCO}_3^-$  to deliver hydroxide in forming  $\text{Mn}(\text{OH})^+$ -apo-WOC, although  $\text{HCO}_3^-$  itself may actually bind. The higher binding affinity of

$\text{Mn(OH)}^+$  over  $\text{Mn}^{2+}$  may represent a selection feature adopted in vivo to enable greater discrimination against more abundant cellular ions like  $\text{Ca}^{2+}$  and  $\text{Mg}^{2+}$  which straddle  $\text{Mn}^{2+}$  in ionic radius.

We have examined several metal ions as potential replacements for  $\text{Mn}^{2+}$  during photoactivation [57]. In these trials, the concentrations of  $\text{Ca}^{2+}$ ,  $\text{Cl}^-$  and protons (pH 6) were not varied but fixed at the optimum values observed with  $\text{Mn}^{2+}$ . So far we have not found evidence for functional replacement of manganese in oxygen evolution by any other metal ion. In all cases studied to date, no photoactivation was observed with any of the following species:  $\text{V}^{3+}$ ,  $\text{VO}^{2+}$ ,  $\text{Cr}^{3+}$ ,  $\text{Fe}^{2+}$ ,  $\text{Fe}^{3+}$ ,  $\text{Co}^{2+}$ ,  $\text{Co(salen)}$ ,  $\text{Ni}^{2+}$ ,  $\text{Cu}^{2+}$ ,  $\text{MoO}_4^-$ ,  $\text{Ru}^{3+}$ ,  $\text{Rh}^{3+}$  and  $\text{Re}^{3+}$ . Some combinations were tried (Mn/Cr, Mn/Fe and Mn/Co) and also showed no additional photoactivation. In the majority of these cases, the alternative metals do bind as competitive inhibitors of  $\text{Mn}^{2+}$  photoactivation. The strongest inhibitors of Mn-dependent photoactivation were either large alkali metal ions like  $\text{Cs}^+$ , or oxo-metal cations like  $\text{UO}_2^{2+}$ , and these targeted the high-affinity  $\text{Mn(OH)}^+$  site [58]. These data suggest that under the restricted conditions examined to date, manganese appears to be truly unique in its capacity to assemble into a functional catalyst for

water oxidation. Other pH conditions need to be examined to have confidence in this generalization. The reason for the unique role of Mn in water splitting is not clear at present. It could be that the correct structure was not assembled or that these other metals do not have the correct thermodynamic properties for water splitting. We note that achieving a sufficient thermodynamic potential for water oxidation (115 kcal/mol per H–OH bond), combined with the need for low  $\text{O}_2$  affinity for the reduced  $\text{Mn}^{n+}$  are features that are found in the  $\text{Mn}^{4+}/\text{Mn}^{2+}$  couple [59].

In the case of the vanadyl ion ( $\text{VO}^{2+}$ ) which does not photoactivate in the absence of  $\text{Mn}^{2+}$ , we observe weak stimulation of Mn-dependent photoactivation at low concentrations ( $< 15 \mu\text{M}$ ) versus inhibition at higher concentrations (50% loss at 210–240  $\mu\text{M}$ ). This two-phase stimulation/inhibition behavior is seen in both the yield of photoactivated centers and the initial lag-time (transit time through the first intermediate  $\text{IM}_1$ ). This two-phase behavior is also observed with other examples of weakly basic electron donors like phenothiazine (pzH) and *N*-hydroxy-L-arginine, as illustrated in Fig. 2 for the latter case and summarized in Table 1 for all examples studied so far. Many weak bases (including also bo-

Table 1

The effect of weak bases and electron donors on the yield of photoactivated centers and initial lag-time of photoactivation (transition time to form  $\text{IM}_1$ )

Additive	50% effect on yield	Effect on lag-time/ $\text{O}_2$ yield	Class	Site <sup>a</sup>
$\text{CO}_2(\text{OH})^-$ (bicarbonate)	$< 25 \mu\text{M}$	shorter/stimulates	aids $\text{Mn}^{2+}$ oxidation weak base stimulator	$\text{IM}_1$
$\text{B(OH)}_4^-$ (borate)	1–2 mM	shorter/stimulates	weak base stimulator	$\text{IM}_1$
DPC <sup>b</sup>	50 $\mu\text{M}$	longer/inhibits	electron donor inhibitor	$\text{Y}_Z$ and $\text{IM}_1$
$\text{NH}_2\text{OH}$	5 $\mu\text{M}$	longer/inhibits	electron donor inhibitor irreversible in light	$\text{Y}_Z$ and $\text{IM}_1$
Formate	300 $\mu\text{M}$	longer/inhibits	electron donor inhibitor	$\text{Y}_Z$ and $\text{IM}_1$
$\text{I}^-$ (iodide)	340 $\mu\text{M}$	no effect/inhibits	electron donor, $\text{Y}_Z$ radical iodination	$\text{Y}_Z$
Trifluoperazine	450 $\mu\text{M}$	longer/inhibits	electron donor inhibitor known calmodulin inhibitor	$\text{IM}_1$ D1 protein?
pzH	10–15 $\mu\text{M}$ 40–45 $\mu\text{M}$	shorter/stimulates increases/inhibits	weak base stimulator electron donor inhibitor	$\text{IM}_1$ $\text{IM}_1$
<i>N</i> -Hydroxyl-L-arginine	15 $\mu\text{M}$ 100–120 $\mu\text{M}$	shorter/stimulates no effect/inhibits	weak base stimulator electron donor inhibitor	$\text{IM}_1$ $\text{Y}_Z$
$\text{VO}^{2+}$	$< 15 \mu\text{M}$ 200 $\mu\text{M}$	shorter/stimulates longer/inhibits	weak base stimulator electron donor inhibitor	$\text{IM}_1$ Ca effector site?

<sup>a</sup>References cited in text.

<sup>b</sup>DPC = diphenylcarbazine.

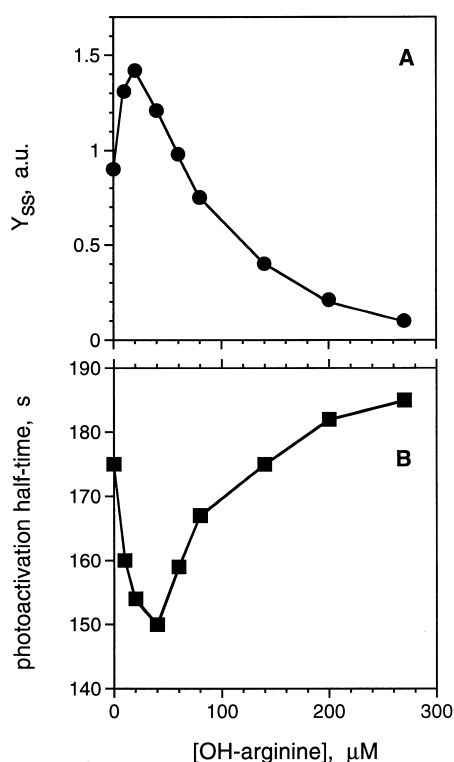


Fig. 2. Effect of *N*-hydroxy-L-arginine on the yield and lag-time for photoactivation of apo-WOC-PSII centers. The data were obtained at a fixed concentration of  $\text{Mn}^{2+}$  and  $\text{Ca}^{2+}$  equal to 8  $\mu\text{M}$  and 10 mM, respectively. Yield data are calculated after attaining the steady-state level  $Y_{\text{SS}}$  from the integrated amplitude of  $\text{O}_2$  produced by pulsed-light excitation. Other conditions as in Fig. 1.

rate, bicarbonate) accelerate Mn-dependent photoactivation without the subsequent inhibition phase by serving solely as proton acceptors (or hydroxide donors). A subset of these like pZH, *N*-hydroxy-L-arginine and  $\text{VO}^{2+}$  also inhibit Mn-dependent photoactivation at higher concentrations by serving as competitive electron donors. Other molecules such as diphenylcarbazide (DPC), hydroxylamine and formate only inhibit by serving as pure electron donors and do not stimulate photoactivation like weak bases. The DPC class of inhibitors has been extensively documented by Ghirardi et al. [60].

A different class of inhibitors of Mn-dependent photoactivation is illustrated by iodide and trifluoperazine (Table 1). Both inhibit by suppression of the yield of photoactivated centers but exert no influence whatsoever on the lag-time for photoactivation. Iodide is a known electron donor directly to  $Y_Z$

[61], that bypasses all assembly intermediates, which explains why it has no effect on an intensive quantity such as the lag-time. Trifluoperazine is a potential electron donor and known inhibitor of calcium-dependent signal transduction proteins belonging to the class of 'EF hand' calcium binding proteins [62]. Its mechanism of inhibition in PSII may also involve either electron donation to oxidized  $Y_Z$ , or possibly a more interesting effect such as blocking of a Ca-dependent conformational change. We have not attempted to resolve these possible mechanisms.

The weak stimulation of Mn-dependent photoactivation by  $\text{VO}^{2+}$ , noted above, disappears at higher calcium concentrations (80 mM) than are needed for saturation of activity (8 mM). We find no evidence that vanadyl alone in the absence of calcium can support Mn-dependent photoactivation, in contrast to a previous report in which vanadyl was able to partially restore activity to the calcium-depleted PSII membrane sample [63]. Our interpretation of the vanadyl stimulation effect is that it interacts with  $\text{Mn}^{2+}$  at the high-affinity site in two ways. It binds to a high-affinity site where it serves as a weak base at pH 6 ( $\text{p}K_1 = 4.3$ ,  $\text{p}K_2 = 11.5$ ) to facilitate deprotonation upon forming  $\text{Mn}(\text{OH})^+$  or possibly  $\text{Mn}(\text{OH})_2^+$  following illumination. Functional replacement of some  $\text{Mn}^{2+}$  by  $\text{VO}^{2+}$  cannot be excluded as a possible interpretation of the stimulation effect, but seems unlikely considering the noted examples of stimulation by weak bases and the complete absence of photoactivation by vanadyl and calcium without manganese. At higher vanadyl concentrations ( $> 20 \mu\text{M}$ ), it inhibits photoactivation by serving as an electron donor ( $E_m = +0.42 \text{ V}$ ,  $\text{VO}^{2+}/\text{VO}^{3+}$ ) to a lower affinity site. Suppression of inhibition from this site occurs at higher concentrations of  $\text{Ca}^{2+}$ , but specific competition vs. non-specific screening was not distinguished. Hence, inhibition may involve either the initial  $\text{Mn}^{2+}$  site or the calcium effector site.

The high-affinity binding sites for the initial  $\text{Mn}^{2+}$  and its  $\text{Mn}^{3+}$  photo-oxidized form have been characterized by EPR. In the reduced  $\text{Mn}^{2+}$  form, it exhibits a surprisingly homogeneous, low-cubic symmetry, ligand field that produces well-resolved zero-field splitting at an effective  $g = 8.3$  value (at 9.3 GHz) and  $^{55}\text{Mn}$  hyperfine structure. These features are consistent with an axial ligand field such as would be expected for  $\text{Mn}(\text{OH})^+$ , although not uniquely attrib-

utable to hydroxide coordination [64]. Campbell et al. identified the EPR signal for the photo-oxidized  $\text{Mn}^{3+}$  using parallel-mode EPR detection [65]. It has been found to exhibit an axially symmetric ligand field with weak rhombicity ( $\sim 10\%$ ), suggested to arise from a square pyramidal or tetragonally distorted octahedral Mn(III) site. Compelling evidence for the involvement of amino acid residue D1-Asp-170 in binding of the Mn ion was given.

### 2.3. Protons

The first photolytic step in photoactivation involves the removal of an electron from the dark  $\text{Mn}(\text{OH})^+$  precursor to yield initially  $\text{Mn}(\text{OH})^{2+}$  followed by proton ionization to yield the first stable intermediate  $\text{Mn}(\text{OH})_2^+$  (Scheme 1). In a previous study, we found that the half-time for photoactivation decreases monotonically with increasing pH between 5.5 and 6.8, indicating that one of the early steps involves release of a proton. From a study of the yield and half-time of photoactivation on buffer concentration, we were able to determine that formation of  $\text{IM}_1$  or  $\text{IM}_2^*$  involves release of  $\geq 1 \text{ H}^+$  into solution [66]. In order to make direct measurements of  $\Delta\text{pH}$  in the sample, we have now introduced an ion-selective field effect transistor (Sentron Corp.) within the  $5 \mu\text{l}$  sample chamber used for pulsed-light photoactivation. Calibration of the proton stoichiometry was performed as shown in Fig. 3, using intact PSII membranes in the presence of ferricyanide as electron acceptor and adoption of the overall stoichiometry:  $2 \text{ H}_2\text{O} + 4 \text{ ferricyanide} \rightarrow \text{O}_2 + 4 \text{ H}^+ + 4 \text{ ferrocyanide}$ . The slope of this plot remains constant for at least 50 flashes provided there is no depletion of electron acceptor. Since ferricyanide does not consume or produce protons upon reduction, the only reaction which produces protons is water oxidation. Accordingly, the slope was set equal to the stoichiometry of one  $\text{H}^+/\text{e}^-$  transferred or four  $\text{H}^+/\text{O}_2$  molecules evolved. In Fig. 3, we show the response from an identical concentration of apo-WOC-PSII sample including all of the inorganic cofactors needed for photoactivation and under identical illumination and buffer capacity conditions. Here we see that the steady-state slope is about three times smaller than native PSII, as would be expected since the rate of proton evolution is limited by the slow step

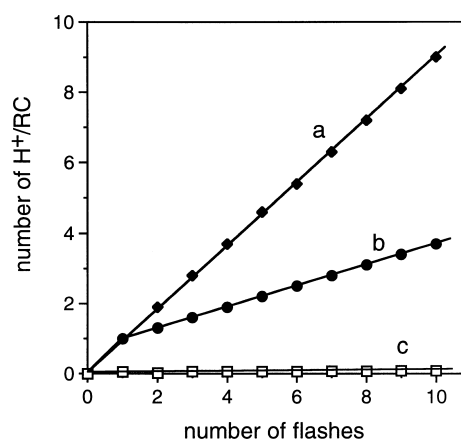


Fig. 3.  $\Delta\text{pH}$  changes caused by blue light flashes applied to (a) intact  $\text{O}_2$ -evolving PSII membranes, (b) apo-WOC-PSII under photoactivation conditions ( $+\text{Mn}^{2+}$ ,  $\text{Ca}^{2+}$ ,  $\text{Cl}^-$ ,  $\text{K}_3\text{FeCN}_6$  as in Fig. 1), and (c) apo-WOC-PSII under photoactivation conditions but in the absence of  $\text{Mn}^{2+}$  and  $\text{Ca}^{2+}$  in assay medium. pH changes were detected using a pH-sensitive field effect transistor (Sentron Corp.) with active area  $\sim 1 \text{ mm}^2$ . Calibration using intact PSII ( $0.5 \mu\text{M}$  of P680) yields a slope of  $0.21 \text{ H}^+/\text{pulse}$  using saturating light intensity at  $472 \text{ nm}$ . Blue excitation flashes provided by LED NSPB500A (Nichia, Japan), at  $30 \text{ ms}$  duration and  $3 \text{ s}$  dark interval.

in photoactivation which is a low quantum yield process [42]. Importantly, the first flash produces one  $\text{H}^+/\text{e}^-$  transferred, corresponding to a stoichiometry of one proton released upon formation of  $\text{IM}_1$  immediately after the flash, or possibly following subsequent binding of  $\text{Ca}^{2+}$  in the dark to give  $\text{IM}_2$ . Control experiments with apo-WOC-PSII centers with  $\text{Mn}^{2+}$  omitted from the medium yield zero net protons on the first flash and zero or weak proton evolution on all subsequent flashes.

### 2.4. Calcium

Calcium is invariably found in all PSII centers and is essential for water oxidation [67]. A stoichiometry of 1–2 calcium has been determined for water oxidation in intact WOC by extraction/reconstitution studies, with more recent works suggesting one  $\text{Ca}/\text{PSII}$  [22]. Removal of calcium from the intact WOC causes a structural change of the  $\text{Mn}_4$  cluster detectable by EPR [68–70], and by a decrease in the binding energy of the Mn core electrons as seen by Mn XANES [71].  $\text{Ca}^{2+}$  removal results in thermodynamic stabilization of the  $\text{Mn}_4$  core in the modified  $\text{S}_2$  and  $\text{S}_3$  states versus the  $\text{S}_1$  state as seen by thermo-

luminescence [72], and also an increased lability for release of  $\text{Mn}^{2+}$  into solution. Extraction/reconstitution studies showed that calcium removal increases access of water molecules and small reductants to the  $\text{Mn}_4$  cluster, supporting a role as ‘gatekeeper’ in restricting small molecule access to the  $\text{Mn}_4$  core [73]. The protein subunits involved in binding of calcium within PSII are not known, but some evidence based on amino acid sequence analysis [74] and also point mutants [75] suggests a role for the A–B loop of the D1 subunit as a potential binding site.

The binding of one calcium ion has been kinetically resolved during assembly of the  $\text{Mn}_4$  core and found to be essential for expression of  $\text{O}_2$  evolution activity upon photoactivation [7].  $\text{Ca}^{2+}$  binding occurs slowly in the dark following the formation of the first light-induced intermediate  $\text{Mn}(\text{OH})_2^+$  ( $\text{IM}_1$ , Scheme 1). The dark calcium-dependent step has a pseudo-first-order rate constant of  $0.0038 \text{ s}^{-1}$  (at  $10 \text{ mM Ca}^{2+}$ ) and is the rate-limiting step overall in assembly at the low concentration of  $\text{Mn}^{2+}$  that is sufficient for saturation of the yield of photoactivation ( $< 10 \mu\text{M}$ ). At low concentration of  $\text{Mn}^{2+}$ , calcium binding to its effector site precedes uptake of the remaining three  $\text{Mn}^{2+}$ . Other data indicate that the sequence of calcium binding may come later in the mechanism if higher  $\text{Mn}^{2+}$  concentrations are used (see later). The calcium requirement appeared to contradict earlier work that found no calcium requirement for assembly, but was restricted to measurements of the yield of photoactivated centers (no kinetic resolution of intermediates) [76]. Resolution of this discrepancy can be reached by considering the molecularity on calcium of each of the first two steps (refer to Scheme 1). In the range of concentrations studied,  $\text{Ca}^{2+}$  accelerates both the second formation step ( $k_2$ ) and the first deactivation step involving  $\text{IM}_1$  ( $k_{-1}$ ). Since the binding constants for  $\text{Ca}^{2+}$  at these two sites are almost the same [7], any measurement based solely on yield that is incapable of kinetically resolving these steps will find no calcium requirement in the assembly process.

Without  $\text{Ca}^{2+}$  present, the apo-WOC-PSII protein binds and photo-oxidizes many more than four  $\text{Mn}^{2+}$  during photoactivation ( $> 10 \text{ Mn}$ ) and fails to express oxygen evolution activity [7,66,76]. Subsequent addition of  $\text{Ca}^{2+}$  in the dark results in rapid recovery of  $\text{O}_2$  activity with no evidence yet for ki-

netically resolved intermediates that precede  $\text{O}_2$  evolution [37,66]. The loss of the slow calcium-dependent step in the presence of the multiply photo-oxidized  $\text{Mn}^{2+}$  ions indicates that there is positive cooperativity between these Mn ions and the uptake of  $\text{Ca}^{2+}$  at its effector site. The origin of the cooperativity is unknown and could indicate either direct bonding through shared ligands or possibly expressed through conformational coupling via the protein.

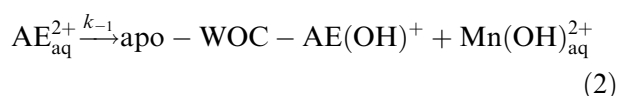
EPR evidence on the interaction between the  $\text{Mn}_4$  core in Ca-depleted PSII and added  $\text{Mn}^{2+}$ , purported to bind to the  $\text{Ca}^{2+}$  site, has been interpreted in favor of distinct (non-overlapping) binding sites for these endogenous cofactors [77]. These studies did not include competition studies showing that added  $\text{Mn}^{2+}$  was bound exclusively at the Ca effector site. The addition of  $\text{Ca}^{2+}$  to a sample of apo-WOC-PSII in the dark was found to induce the binding of more  $\text{Mn}^{2+}$  from solution than to controls having  $\text{Ca}^{2+}$  replaced by  $\text{Mg}^{2+}$  or  $\text{Na}^+$  [64]. The  $\text{Mn}^{2+}$  ions that were induced to bind by the presence of  $\text{Ca}^{2+}$  were identified by EPR to be interacting via spin-exchange coupling and thus bound to a binuclear site in close proximity to each other (ca.  $4 \text{ \AA}$ ). This calcium-induced binuclear  $\text{Mn}_2(\text{II},\text{II})$  center was capable of efficient electron donation to photo-oxidized  $\text{Y}_Z$  and also photoactivated immediately without a kinetic lag-time. These data suggest that calcium can participate in forming the binding site for at least two of the four Mn ions. These results differ from the conclusions derived from equilibrium binding studies by Ono and Mino showing that  $\text{Ca}^{2+}$  or  $\text{Mg}^{2+}$  prevented excess  $\text{Mn}^{2+}$  from binding to apo-WOC with the exception of one Mn/RC [78]. These studies did not determine whether the bound  $\text{Mn}^{2+}$  was uniformly distributed or in the form of spin-coupled clusters of two or more Mn ions. These results are related to earlier work by Kulikov et al. on the magnetic dipolar interaction of reconstituted Mn(II) ions bound to apo-WOC-PSII with the pheophytin anion radical. The authors proposed the existence of intermanganese spin-coupling in the initial two pairs of Mn(II) ions to account for reduced magnetic interaction with the pheophytin anion radical in the presence of two and four but not one and three Mn/RC [79].

$\text{Ca}^{2+}$  is the only metal ion that binds to the cal-

cium effector site in vivo in all native O<sub>2</sub>-evolving organisms studied to date. Boussac and Rutherford established the conditions for exchanging Ca<sup>2+</sup> for strontium in intact PSII membranes without prior removal of manganese [80]. Sr<sup>2+</sup> replacement was shown to support a maximum steady-state O<sub>2</sub> evolution rate that is 30% of the calcium-dependent rate. All PSII centers are reconstituted by Sr<sup>2+</sup> and the lower rate reflects a decrease in the rate of the final S-state transition (S<sub>3</sub> → S<sub>0</sub> + O<sub>2</sub>). Cadmium was also reported to bind, as seen by restoration of normal thermoluminescence, but did neither restore O<sub>2</sub> evolution nor the normal EPR signatures for the S<sub>2</sub> state [68].

We have examined the possibility of Sr<sup>2+</sup> replacing Ca<sup>2+</sup> during photoactivation of apo-WOC-PSII where competition between the Mn and Ca<sup>2+</sup> sites can be assessed directly by kinetic measurements of the three pseudo-first-order rate constants ( $k_1$ ,  $k_{-1}$  and  $k_2$ ) (Scheme 1). Rate constant measurements were performed as described in Zaltsman et al. [7]. Previous work showed that the  $k_1$  step of photoactivation is independent of the Ca<sup>2+</sup> concentration in the medium, first-order in Mn<sup>2+</sup> concentration and first-order in OH<sup>-</sup> concentration [20]. Thus we did not expect to see a dependence on Sr<sup>2+</sup> and this was indeed confirmed. The data for the inactivation of the first intermediate,  $k_{-1}$ , are shown in Fig. 4A, where it is seen that both Sr<sup>2+</sup> and Ca<sup>2+</sup> accelerate the rate of decay of IM<sub>1</sub> with a first-order dependence, i.e.  $k_{-1} = k_{\text{obs}}[\text{AE}^{2+}]^1$ , AE (alkaline earth) = Ca or Sr. This behavior was previously attributed to the bimolecular deactivation of IM<sub>1</sub> by AE<sup>2+</sup> [7]. Eq. 2 presents the net reaction including the new proton stoichiometry given herein and the thermodynamic data showing that binding of AE(OH)<sup>+</sup> (rather than AE<sup>2+</sup>) occurs in competition with Mn(OH)<sup>+</sup> [58].

Apo – WOC – Mn(OH)<sub>2</sub><sup>+</sup> +



The slopes of the rates in Fig. 4 also demonstrate that this deactivation process is 5-fold slower for Sr<sup>2+</sup> than for Ca<sup>2+</sup>. This slower rate may be partially rationalized on the basis of the higher binding affin-

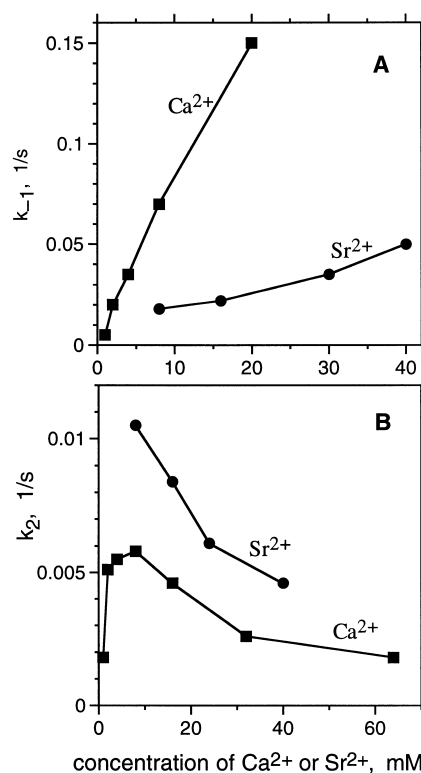


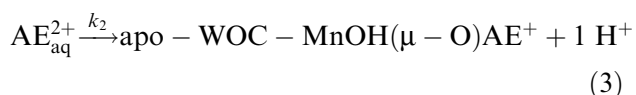
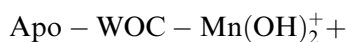
Fig. 4. Rate constants: (A)  $k_{-1}$  for decay of the first light-induced intermediate IM<sub>1</sub> formed during photoactivation of apo-WOC-PSII in the presence of Ca<sup>2+</sup> or Sr<sup>2+</sup> in the medium; and (B)  $k_2$  for formation of the dark intermediate IM<sub>2</sub> during photoactivation of apo-WOC-PSII in the presence of Ca<sup>2+</sup> or Sr<sup>2+</sup> in the medium.

ity for hydroxide observed for Ca<sub>aq</sub><sup>2+</sup> vs. Sr<sub>aq</sub><sup>2+</sup>, log  $K(\text{hydrolysis}) = 1.4$  vs. 0.6.

Fig. 4B compares the dependence of the (overall rate-limiting) step  $k_2$  on Ca<sup>2+</sup> and Sr<sup>2+</sup> concentrations. A first-order stimulation of the rate by calcium occurs below 8 mM, which was the basis for assigning a single Ca<sup>2+</sup> in the slow step of photoactivation [7]. Above this concentration, excess Ca<sup>2+</sup> weakly inhibits photoactivation, as do many other ions including Na<sup>+</sup>, Mg<sup>2+</sup>, Ba<sup>2+</sup> and Sr<sup>2+</sup>. Accordingly, this inhibition was attributed to general electrostatic screening. By varying the length of the dark period between flashes, the  $k_2$  step was shown to be a dark process (no photons needed) and was much slower than the longest dark interval tested (10 s).

Photoactivation of apo-WOC-PSII is indeed observed with Sr<sup>2+</sup> replacing Ca<sup>2+</sup>. The final O<sub>2</sub> yield per single turnover flash was found to be 30% at the optimum concentration (50 mM) relative to 100% for

the  $\text{Ca}^{2+}$  control at its optimum concentration (8 mM) (not shown). These results are essentially identical to the earlier works using Ca-extracted/Sr-substituted intact PSII samples. The same weak inhibition of the  $\text{Sr}^{2+}$ -dependent  $k_2$  rate is also seen at high  $\text{Sr}^{2+}$  concentrations (Fig. 4B). It is more difficult to examine the kinetics with  $\text{Sr}^{2+}$  owing to the lower  $\text{O}_2$  activity, hence the data set could not be extended below 8 mM. Nevertheless, Fig. 4B shows that at all  $\text{Sr}^{2+}$  concentrations the rate of formation of  $\text{IM}_2$  is faster with  $\text{Sr}^{2+}$  vs.  $\text{Ca}^{2+}$ . It is two times faster at 8 mM and may be even faster at lower concentrations as suggested by the trend. The faster rate-limiting  $k_2$  step with  $\text{Sr}^{2+}$  may be interpreted in terms of either a faster protein conformational step or, alternatively, a faster binding rate for  $\text{Sr}^{2+}$  to the  $\text{Mn}(\text{OH})_2^+$  precursor in  $\text{IM}_1$  via a mechanism involving bridge formation, Eq. 3



In Eq. 3, we suggest the possibility that a  $\mu$ -oxide or  $\mu$ -hydroxide bridge forms between  $\text{Mn}^{3+}$  and  $\text{AE}^{2+}$  involving one or both of the hydroxo ligands in  $\text{IM}_1$ , possibly accompanied by proton release into solution. This step would produce the oxide bridges considered essential for high-affinity binding of the remaining three  $\text{Mn}^{2+}$  in subsequent photoactivation steps leading to the functional  $\text{Mn}_4$  cluster. At present, we do not have definitive evidence distinguishing these two possibilities (or others) for the mechanism of the rate-limiting  $k_2$  step. However, it seems unlikely that protein conformational change would be slower with  $\text{Ca}^{2+}$  than  $\text{Sr}^{2+}$  since the metal charge density favors higher affinity for the smaller Ca. Desolvation of  $\text{AE}^{2+}$  also could not be rate-limiting as it is many orders of magnitude faster than  $k_2$  [81]. On the other hand, Eq. 3 predicts that the  $k_2$  step in assembly should accelerate under alkaline conditions. No studies are available yet of the pH dependence of  $k_2$  which could test this hypothesis. The proton evolution studies reported above showed that one proton is evolved immediately following the first flash in forming  $\text{IM}_1$ , but did not examine the extent of additional proton release in the following

slow dark process or its dependence on  $\text{Ca}^{2+}$  concentration.

We also performed photoactivation studies attempting to replace  $\text{Ca}^{2+}$  with other alkaline earth ions, including  $\text{Mg}^{2+}$  and  $\text{Ba}^{2+}$ . Neither ion was found capable of supporting photoactivation in place of  $\text{Ca}^{2+}$ . As noted above,  $\text{Mg}^{2+}$  weakly inhibits photoactivation at a low-affinity (non-specific) site. By contrast,  $\text{Ba}^{2+}$  proved to be an inhibitor, not at the calcium site, but rather by competition with  $\text{Mn}^{2+}$  in the formation of the first intermediate ( $\text{IM}_1$ ).

In summary,  $\text{Sr}^{2+}$  is much better for photoactivation kinetics than is  $\text{Ca}^{2+}$ , both by accelerating the rate-limiting step in assembly ( $k_2$ ) and retarding the deactivation of the first intermediate ( $k_{-1}$ ). This result suggests that there is no reason why plants and algae that utilize  $\text{Sr}^{2+}$  instead of  $\text{Ca}^{2+}$  could not exist in vivo. The uptake of  $\text{Sr}^{2+}$  by marine plants is quite high and even greater than  $\text{Ca}^{2+}$  when expressed as the fractional enrichment relative to the sea concentration (32–173-fold increase for Sr (8 ppm seawater) vs. 25-fold for Ca (400 ppm seawater) [6]). Perhaps by looking in areas where the local natural abundance of these elements favors  $\text{Sr}^{2+}$ , one might find a ‘strontium mutant’. The kinetic preference of the calcium effector site for  $\text{Sr}^{2+}$  vs.  $\text{Ca}^{2+}$  makes sense biologically too, if one considers that in vivo this site must selectively bind  $\text{Ca}^{2+}$  in the presence of divalent cations like  $\text{Mn}^{2+}$ ,  $\text{Mg}^{2+}$  and  $\text{Zn}^{2+}$ .  $\text{Mn}^{2+}$  has the same charge, spherically symmetrical electronic configuration and is only 20% smaller in ionic radius vs.  $\text{Ca}^{2+}$  (1.0 Å).  $\text{Mg}^{2+}$  is considerably smaller (0.65 Å radius) but is relatively abundant in vivo. Consequently, nature may have tuned the calcium effector site so that thermodynamically it prefers to bind the larger  $\text{Sr}^{2+}$  ion (1.13 Å radius) with higher affinity than  $\text{Ca}^{2+}$ . This selectivity would suppress competition from smaller more abundant ions like  $\text{Zn}^{2+}$  and  $\text{Mg}^{2+}$ , as well as  $\text{Mn}^{2+}$ . Discrimination against  $\text{Mn}^{2+}$  binding to the calcium effector site is critical as otherwise it short-circuits functional assembly by inducing photo-ligation/oxidation of large amounts of  $\text{Mn}^{2+}$  [7,76].

Following the uptake of calcium at its effector site in the dark  $k_2$  step of photoactivation, there is a large increase in the quantum yield for stable photo-oxidation of  $\text{Mn}^{2+}$  in the next photoactivation step [7]. Although this step and subsequent steps

are faster and have not been kinetically resolved yet, it is clear that calcium contributes importantly to enhancing the probability of stable photo-oxidation of the second  $\text{Mn}^{2+}$  in forming  $\text{IM}_2$ . The enhanced stability of the second intermediate was originally noted by Chéniaie's group, although calcium was not known to be involved then [37,42]. We estimate that, at the concentrations stated in the legend to Scheme 1, the slowest of these steps must occur at least two times faster than the rate-limiting dark  $k_2$  step, based on numerical modeling results of the overall process of  $\text{O}_2$  recovery using a standard, mass-action, three-step, kinetic model (Gepasi WEB-based software; P. Mendes). Based on the above evidence, we have previously proposed a structural model for  $\text{IM}_2$  as a calcium-induced spin-coupled dimanganese(III,III) species, possibly containing bridging oxos or hydroxos (Scheme 1). This proposal would be compatible with EPR studies showing that calcium induces binding of two Mn(II) ions to apo-WOC-PSII in the dark which form a spin-coupled dimanganese(II,II) center (see Section 2.2) [64]. Subsequently,  $\text{IM}_2$  binds two additional  $\text{Mn}^{2+}$  ions and an unknown number of  $\text{Cl}^-$  ions and possibly absorbs additional photons to complete formation of the functional  $\text{Mn}_4\text{Ca}_1\text{Cl}_x$  cluster. Since only one  $\text{Ca}^{2+}$  site has been identified for loss of  $\text{O}_2$  evolution activity and only one  $\text{Ca}^{2+}$  ion is kinetically revealed in reconstitution of activity during photoactivation, there is no evidence to suggest that another  $\text{Ca}^{2+}$  is taken up following binding to the calcium effector site.

In conclusion, these data and the literature summarized above indicate the following roles for calcium in both assembly and water oxidation: (1) creation of the second (and subsequent?)  $\text{Mn}^{2+}$  binding sites while also increasing the quantum yield for their stable photo-oxidation, (2) eliminating the coordination of excess  $\text{Mn}^{2+}$  (beyond four Mn/RC), (3) limiting the accessibility of substrate molecules and small reductant molecules to the  $\text{Mn}_4$  core, and (4) activation of the substrate during the  $\text{O}_2$  evolution step ( $\text{S}_3 \rightarrow \text{S}_0$ ). The majority of kinetic and spectroscopic studies indicate a cooperativity in physico-chemical properties and also a close physical proximity between the  $\text{Mn}_4$  cluster and calcium in the WOC. This conclusion is not universal, but it is also consistent with the interpretation of Sr EXAFS data on

$\text{Ca}^{2+}$ -depleted/ $\text{Sr}^{2+}$ -reconstituted PSII membranes suggesting an Mn–Sr distance of 3.5 Å [71]. Recent  $^{113}\text{Cd}$  solid-state NMR studies of  $\text{Ca}^{2+}$ -depleted/ $\text{Cd}^{2+}$ -exchanged PSII membranes gave evidence for efficient magnetic dipolar relaxation of the Cd nucleus that was attributed to coupling with the  $\text{Mn}_4$  cluster (dark  $\text{S}_1$  state) [82]. These data were also interpreted in favor of a close association of these two centers. Clearly, more work needs to be done to pinpoint the location of the calcium site in PSII and the mechanistic details of how it activates the substrate for  $\text{O}_2$  evolution.

Lastly, Scheme 1 depicts a possible structure for the functional WOC in the  $\text{S}_0$  state, which we have previously formulated as containing Mn oxidation states of II,III<sub>3</sub> based on extrapolation of the EPR data for the  $\text{S}_2$  state [83]. The structure of the core geometry is under extensive debate by several groups. We have presented evidence for an incomplete cubane type core structure  $\text{Mn}_4\text{O}_2\text{X}_2$  ( $\text{X} = \text{Cl}^-, \text{OH}^-, \text{OH}_2$ ) analogous to that suggested in Scheme 1, based on a model  $\text{Mn}_4$ -cubane core complex [84]. Further discussion of the evidence for this core type in PSII is summarized in Section 3.

## 2.5. Chloride

Based on a variety of indirect lines of evidence on reconstituted systems, the location of the functional chloride binding site(s) within the WOC is conjectured to be on Mn. However, unambiguous spectroscopic localization to  $\text{Mn}^{n+}$ ,  $\text{Ca}^{2+}$  or any other Lewis acid site has not yet been proven by compelling data. The mean binding affinity is weak when assayed by steady-state  $\text{O}_2$  evolution rates ( $K_M \sim 1$  mM) and found to be S-state-dependent when monitored by dynamic  $^{35}\text{Cl}^-$  NMR lineshape changes [85]. The latter NMR binding data and also UV-Vis absorption changes monitoring S-state transitions attributed to Mn absorption were found to indicate functional binding of  $\text{Cl}^-$  in the  $\text{S}_2$  and  $\text{S}_3$  states that was essential for the photo-conversion to the  $\text{S}_3$  and  $\text{S}_0$  states, respectively. By contrast, no functional  $\text{Cl}^-$  binding nor requirement for S-state transitions was seen in  $\text{S}_0$  or  $\text{S}_1$  [86,87]. The interpretation of the NMR studies showing no  $\text{Cl}^-$  binding in the lower S-states is not supported by equilibrium binding data, including radioactive  $^{36}\text{Cl}^-$  studies on the

dark  $S_1$  state showing a high-affinity site ( $K_D \sim 20 \mu\text{M}$ ) [23]. EPR data also indicate a requirement for  $\text{Cl}^-$  for enabling charge transfer to produce the normal  $S_3$  state (Mn oxidation?) from  $S_2Y_Z^*$  in  $\text{Cl}^-$ -depleted samples [88] or  $\text{F}^-$ -substituted samples [89]. A small number of anions appear to be able to replace chloride in water oxidation/oxygen evolution, albeit with lower specific activity ( $\text{Cl}^- > \text{Br}^- > \text{NO}_3^-$ , etc.). Certain inhibitory treatments of PSII like  $\text{Ca}^{2+}$  depletion or removal of  $\text{Cl}^-$  or replacement by  $\text{F}^-$  or by acetate lead to a structural change of the  $\text{Mn}_4$  cluster (detected in  $S_2$ ), with complete loss of  $\text{O}_2$  evolution activity. Force et al. estimated by pulsed EPR methods that acetate binds close to the WOC (ca.  $3.5 \text{ \AA}$ ) in the inhibited  $S_2Y_Z^*$  state formed at high acetate concentrations (0.3 M). Since acetate binds competitively with  $\text{Cl}^-$ , this was interpreted in terms of a model in which  $\text{Cl}^-$  is located close to both  $Y_Z$  and Mn [90]. However, determination of competition between ions that bind to a membrane protein site is subject to strong interference effects from the Donnan potential at such high acetate concentrations, and this complication was not considered in the interpretation of the apparent competition.

Loss of  $\text{O}_2$  evolution upon removal of  $\text{Cl}^-$  or replacement by  $\text{F}^-$  or by  $\text{Ca}^{2+}$  depletion leads to an aborted reaction, the photo-production of hydrogen peroxide from water. The normal  $S_2 \rightarrow S_3$  and  $S_3 \rightarrow S_0$  steps are completely blocked and substrate oxidation (and therefore water binding) proceeds in these inhibited samples in the  $S_2$  state. Production of  $\text{H}_2\text{O}_2$  from water is thermodynamically much more difficult than  $\text{O}_2$  evolution (by 0.5 V per electron), but involves only a two-electron oxidation process. The accumulated evidence can be interpreted to indicate that binding of the functional chloride enables hole transfer within the  $\text{Mn}_4$  cluster to the Mn ions that are least involved in substrate water activation, thus blocking premature substrate oxidation in the native  $S_2$  and  $S_3$  states. The data are consistent with an earlier hypothesis in which chloride serves to promote electron transfer between the Mn ions [91,92]. In one expression of this model that was described previously [93],  $\text{Cl}^-$  induces intra-manganese electron transfer, in contrast to  $\text{F}^-$ - or  $\text{OH}^-$ -exchanged WOC, by increasing the reduction potential of the gateway Mn(IV) ion (closest Mn to  $Y_Z^*$ ) relative to the distal Mn(III) ions, specifically in the

$S_2$  and  $S_3$  states. The higher reduction potential ensures transfer of the hole from the gateway Mn(IV) site to one of the distal Mn(III) ions in normal centers, rather than performs the aborted two-electron oxidation of water. In support of this view, the electrochemical studies of Mn(III,IV) model complexes having  $\text{Cl}^-$  ligands vs.  $\text{OH}^-$  ligands do show appreciably higher reduction potentials [94]. This model argues in favor of a central role for the gateway Mn ion in substrate activation.

### 3. Substrate (water) and ligand sites

Various lines of evidence, recently summarized by Debus [50], have accumulated indicating that the terminal ligands to the Mn ions include at least one histidine ligand [35,36,38,95–97] with a majority of oxygen donor ligands such as protein carboxylate. Either the oxo-bridges or more labile (terminal?) sites on Mn, possibly as hydroxide ions or water molecules, must be the penultimate substrates. But compelling evidence implicating one type of site over another as the substrate site is still lacking. Oxide bridges ( $\text{O}^{2-}$ ) bound between Mn ions comprising two weakly interaction pairs of rhombohedral  $\text{Mn}_2\text{O}_2$  cores (the dimer-of-dimers structural mode) have been proposed in the  $S_1$  and  $S_2$  states on the basis of comparison of intermanganese scattering distances in  $\text{Mn}_2\text{O}_2$  model complexes as determined by Mn EXAFS [98]. However, direct evidence for the putative oxo-bridges is weak. Indirect evidence for oxygen donor ligands to Mn also includes the absence of appreciable Mn–ligand hyperfine couplings in the  $S_2$  state (reviewed in [25]).

Recent Mn EXAFS data have indicated that the intermanganese separations increase by 0.1–0.3  $\text{ \AA}$  in the  $S_3$  state [99]. The longer of the two distances (2.8  $\text{ \AA}$  and 3.0  $\text{ \AA}$ ) is considerably longer than observed in any of the numerous dimanganese model complexes having the  $\text{Mn}_2\text{O}_2^{n+}$  core [100], but is very close to the distance found in the symmetrical  $\text{Mn}_4\text{O}_4^{6+}$  ‘cubane’ core compounds (2.95  $\text{ \AA}$ ) [16]. The EXAFS data were interpreted in favor of oxidation of an oxide bridge to an oxyl radical in one of the  $\text{Mn}_2\text{O}_2$  cores in  $S_3$ , a process not yet shown to occur in any of the dimanganese model complexes to date. The dimer-of-dimers structural model for the  $\text{Mn}_4$  core

has been challenged as incapable of accounting for the basic magnetic properties of the  $S_2$  state [83,101,102]. An alternative structural model that is consistent with both the magnetic data and some of the Mn EXAFS data for the  $S_3$  state is an, incomplete, cubane core such as  $Mn_4O_2(OH)Cl^{8+}$  or  $Mn_4O_2(OH)_2^{8+}$ , which have two bridges different from oxides resulting in local  $C_2$  symmetry. We also note that the trigonal symmetry in complete cubanes of core type  $Mn_4O_3X^{6+}$  has intermediate-spin ground states ( $S=9/2$ ) that are not consistent with the low-spin ground state for the  $S_0$  and  $S_2$  states of OEC [103]. The latter core type has been implicated as an intermediate in the reductive dehydration of the  $Mn_4O_4$ -cubane core complexes that form the  $Mn_4O_2$ -‘pinned butterfly’ core complexes as summarized in Eq. 1 [18]. A structural representation of a reduced precursor to this core type for the  $S_0$  state is depicted in Scheme 1. Stoichiometric  $O_2$  release has also been reported from  $Mn_4O_4^{6+}$  cubane core compound that rearranges to  $Mn_4O_2^{6+}$  ‘butterfly’ [17]. A proposal for how calcium might facilitate an analogous rearrangement in the WOC has been presented [84]. The relationship of this model chemistry to the enzyme remains to be examined in more detail. Many other proposals have been advanced for the mechanism of water oxidation in PSII (see this volume).

A new perspective on water oxidation chemistry has come from studies of the dynamics of substrate water exchange rates measured by time-resolved mass spectrometry. Wydrzynski’s group has pioneered these measurements [104–106]. Their data for the  $S_0$  through  $S_3$  states in PSII membranes are given in Table 2, and the same basic behavior was

also observed in intact thylakoids and PSII core particles. Their kinetic data could be fitted to two populations having different exponential exchange rates in each S-state, with both the fast and slow sites involving comparable fractions approaching 50% each. These data have been interpreted to indicate the presence of only two binding sites, one for each of the two substrate molecules, and that there is no irreversible step in water splitting prior to  $S_4$ . Thus the irreversible step in catalysis – presumed to involve the initial O–O bond formation step – occurs on the final step ( $S_4 \rightarrow S_0$ ). These data confirm the original hypothesis by Kok and coworkers that water oxidation appears to involve an ‘all-or-nothing’ (concerted) four-electron oxidation process that commences in  $S_4$  [107].

The mass spectrometry data show that the lability of the two substrate sites is clearly very different in all S-states with one site in rapid exchange with bulk water (essentially kinetically irresolvable) and the other site being  $100$ – $10^4$  slower. The authors suggest an interpretation of the data in terms of a model in which water binds to two independent Mn(III) ions that are also the catalytic Mn sites, but separate from the Mn ions involved in storage of oxidizing equivalents. They argue that the oxidation states of both of these Mn(III) ions never change during S-state advancement from  $S_0$  to  $S_3$ , to account for the relatively small dependence of rate on S-states (ignoring the 100 times slower  $S_1$  rate). Reasonable but non-unique alternative interpretations for the exchange rates can be offered based on water exchange data for model complexes [81]. The slow exchanging water molecule might also be consistent with binding to a bridging position between two or more metal ions, Mn–(OH)–Mn or Mn–(OH)–Ca. The faster exchanging water molecule might instead be bound terminally as  $Ca^{2+}(OH_2)\dots X$  or  $Mn^{n+}(OH_2)\dots X$  in which additional kinetic retardation is imposed through hydrogen bonding to a protein residue (X).

The  $100$ – $1000$ -fold slower exchange rate in  $S_1$  vs. the  $S_0$  and  $S_2$  states is remarkable. Its significance remains unexplained. One hypothesis to consider is that it may play a physiological role in protecting PSII against disassembly of the WOC and release of  $Mn^{2+}$  initiated by reaction of the  $S_1$  state  $Mn_4$  core with diffusible reductants that are present in the chloroplast ( $H_2O_2$ , ascorbate, glutathione).

Table 2  
PSII WOC water exchange rate constants<sup>a</sup> and hydrogen peroxide dismutation rate constant (catalase)<sup>b</sup>

S-state	H <sub>2</sub> O exchange rates <sup>a</sup> (s <sup>-1</sup> )		Catalase rate constant <sup>b</sup> (s <sup>-1</sup> )
	slow	fast	
$S_0$	8–18	> 100	< 0.007
$S_1$	0.02	> 100	0.4
$S_2$	2	> 175	
$S_3$	2	37	

<sup>a</sup>10°C, pH 6.8 [104–106].

<sup>b</sup>25°C, pH 6.5 [108].

Exogenous hydrogen peroxide ( $\text{H}_2\text{O}_2$ ) also binds to the WOC and produces  $\text{O}_2$  and  $\text{H}_2\text{O}$  in the dark via a dismutation reaction (so-called catalase activity) [108–112]. The reaction involves two distinct catalytic cycles between  $\text{S}_2$  and  $\text{S}_0$  and also between  $\text{S}_1$  and  $\text{S}_{-1}$ . The rate constant for the  $\text{S}_2/\text{S}_0$  cycle ( $0.4 \text{ s}^{-1}$ ) can easily be measured after producing  $\text{S}_2$  by a single turnover flash from dark  $\text{S}_1$ , while only an upper limit for the rate constant for the dark  $\text{S}_1/\text{S}_{-1}$  cycle ( $<0.007 \text{ s}^{-1}$ ) could be determined [113]. It is interesting to note that the 100-fold decrease in the catalase rate constant observed for the  $\text{S}_1$  vs.  $\text{S}_2$  states exactly mirrors the change in the slower rate constant for the substrate water exchange reaction in these S-states observed by Hillier et al. (Table 2). On this basis, we postulate that the exogenous peroxide binding site (catalase site) may be equivalent to (or in equilibrium with) the slowly exchanging substrate water binding site. Mano et al. reported the Michaelis constant for  $\text{H}_2\text{O}_2$  dismutation by the  $\text{S}_2/\text{S}_0$  states to be 10–15 mM at pH 6.5, and that inhibition occurred by small neutral acids with stronger inhibition by the weaker acids at fixed pH [108]. The reported trend in inhibitor effectiveness,  $\text{HCN} \gg \text{HF} > \text{HCl}$ , correlates the strongest inhibition with the unique conjugate anion ( $\text{CN}^-$ ). Cyanide binds to terminal sites on metal ions almost exclusively via its single lone-pair of electrons on carbon, while  $\text{Cl}^-$  and  $\text{F}^-$  can bind at both terminal and bridging metal sites. This correlation suggests that the peroxide binding site and, by this postulate, also the slowly exchanging substrate site in  $\text{S}_2/\text{S}_0$  have the characteristics of a terminal (i.e. non-bridging) manganese coordination site. Catalase activity is invariably associated with direct coordination of peroxide to manganese in both the authentic catalases and their dimanganese model complexes [114].

Mano et al. [113] also found that the inhibition activity of the  $\text{S}_2/\text{S}_0$  catalase site is very different than inhibition at the functional chloride site(s) that is essential for water oxidation/ $\text{O}_2$  evolution. Thus, if the catalase site and the slow substrate site are indeed the same site as suggested above, then the slow substrate site must also be distinct from the functional chloride site. The possibility that the fast exchanging substrate site may exchange with the functional  $\text{Cl}^-$  site is not precluded nor required by this model.

## Acknowledgements

We thank Dr. R. Watt for several helpful comments on the text and Drs. T. Wydrzynski, W. Hillier, Y. Abe, V. Klimov, S. Baranov, A. Boelrijk and C. Tommos for discussions and Mr. R. McInturff and E. Bruntrager for preliminary studies. Research supported by the NIH (Grant GM39932).

## References

- [1] P.G. Falkowski and J.A. Raven, *Aquatic Photosynthesis*, Blackwell, Malden, 1997.
- [2] R.E. Blankenship, H. Hartman, *Trends Biochem. Sci.* 23 (1998) 94–97.
- [3] M. Kagawa, Y. Nichikawa, G. Matsumoto, Y. Kurata, T. Mizobata, Y. Kawata, J. Nagai, *Arch. Biochem. Biophys.* 362 (1999) 346–355.
- [4] T. Igarashi, Y. Kono, K. Tanaka, *J. Biol. Chem.* 271 (1996) 29514–29521.
- [5] S.V. Baranov, G.M. Ananyev, V.V. Klimov, G.C. Dismukes, *Biochemistry* 39 (2000) 6060–6065.
- [6] H.J.M. Bowen, *Trace Elements in Biochemistry*, Academic, New York, 1966.
- [7] L. Zaltsman, G. Ananyev, E. Bruntrager, G.C. Dismukes, *Biochemistry* 36 (1997) 8914–8922.
- [8] H.D. Holland, *Chemical Evolution of the Atmosphere and Oceans*, Princeton University Press, Princeton, NJ, 1984.
- [9] E.R. Stadtman, P.B. Berlett, P.B. Chock, *Proc. Natl. Acad. Sci. USA* 87 (1990) 384–388.
- [10] S.I. Allakhverdiev, I. Yruela, R. Picorel, V.V. Klimov, *Proc. Natl. Acad. Sci. USA* 94 (1997) 5050–5054.
- [11] V.V. Klimov, S.I. Allakhverdiev, Y.M. Feyziev, S.V. Baranov, *FEBS Lett.* 363 (1995) 251–255.
- [12] V.V. Klimov, S.V. Baranov, R. Hulsebosch, S.I. Allakhverdiev, H. Wncencjusz, H. van Gorkom, A. Hoff, *Biochemistry* 36 (1997) 16277–16281.
- [13] V.V. Klimov, S.V. Baranov, S.I. Allakhverdiev, *FEBS Lett.* 48 (1997) 243–246.
- [14] V.V. Klimov, S.I. Allakhverdiev, S.V. Baranov, Y.M. Feyziev, *Photosynth. Res.* 46 (1995) 219–225.
- [15] W.F. Ruettinger, D.M. Ho, G.C. Dismukes, *Inorg. Chem.* 38 (1999) 1036–1037.
- [16] W. Ruettinger, C. Campana, G.C. Dismukes, *J. Am. Chem. Soc.* 119 (1997) 6670–6671.
- [17] W. Ruettinger, M. Yagi, K. Wolf, S. Bernasek and G.C. Dismukes, *J. Am. Chem. Soc.* (2000) (in press).
- [18] W.F. Ruettinger, G.C. Dismukes, *Inorg. Chem.* 39 (2000) 1021–1027.
- [19] R.J. Debus, *Biochim. Biophys. Acta* 1102 (1992) 269–352.
- [20] G.M. Ananyev, G.C. Dismukes, *Biochemistry* 35 (1996) 4102–4109.
- [21] K.-C. Han, S. Katoh, *Plant Cell Physiol.* 34 (1993) 585–593.

- [22] P. Adeloeth, K. Lindberg, L.-E. Andreasson, *Biochemistry* 34 (1995) 9021–9027.
- [23] K. Lindberg, L.-E. Andreasson, *Biochemistry* 35 (1996) 14259–14267.
- [24] K. Lindberg, T. Vanngard, L.-E. Andreasson, *Photosynth. Res.* 38 (1993) 401–408.
- [25] R.D. Britt, in: D.R. Ort and C.F. Yocum (Eds.), *Oxygenic Photosynthesis—The Light Reactions*, Vol. 4, Kluwer, Dordrecht, 1996, pp. 137–164.
- [26] X.-S. Tang, M. Sivaraja, G.C. Dismukes, *J. Am. Chem. Soc.* 115 (1993) 2382–2389.
- [27] T.A. Ono and Y. Inoue, in: Y. Inoue et al. (Eds.), *The Oxygen Evolving System of Photosynthesis*, Academic Press, 1983, pp. 337–344.
- [28] G.M. Ananyev, M.A. Shafiev, V.V. Klimov, *Biophysics (Russia)* 33 (1988) 637–643.
- [29] B.-D. Hsu, J.-Y. Lee, R.-L. Pan, *Biochim. Biophys. Acta* 890 (1987) 89–96.
- [30] G.M. Ananyev, M.A. Shafiev, T.V. Isaenko, V.V. Klimov, *Biophysics (Russia)* 33 (1988) 285–289.
- [31] A.-F. Miller, G. Brudvig, *Biochemistry* 28 (1989) 8181–8190.
- [32] M. Miyao, Y. Inoue, *Biochim. Biophys. Acta* 1056 (1991) 47–56.
- [33] T. Yamashita and A. Ashizawa, in: Y. Inoue et al. (Eds.), *The Oxygen Evolving System of Photosynthesis*, Academic Press, 1983, pp. 327–336.
- [34] C.W. Hoganson, D.F. Ghanotakis, G.T. Babcock, C.F. Yocum, *Photosynth. Res.* 22 (1989) 285–293.
- [35] C. Preston, M. Seibert, *Biochemistry* 30 (1991) 9615–9624.
- [36] C. Preston, M. Seibert, *Photosynth. Res.* 22 (1989) 101–113.
- [37] N.Y.I. Tamura, G.M. Cheniae, *Biochim. Biophys. Acta* 976 (1989) 173–181.
- [38] N. Tamura, M. Ikeuchi, Y. Inoue, *Biochim. Biophys. Acta* 973 (1989) 281–289.
- [39] N. Tamura, H. Kamachi, N. Hokari, H. Masumoto, H. Inoue, *Biochim. Biophys. Acta* 1060 (1991) 51–58.
- [40] M.L. Ghirardi, C. Preston, M. Seibert, *Biochemistry* 37 (1998) 13567–13574.
- [41] M.L. Ghirardi, T.W. Lutton, M. Seibert, *Biochemistry* 37 (1998) 13559–13566.
- [42] N. Tamura, G.M. Cheniae, *Biochim. Biophys. Acta* 890 (1987) 179–194.
- [43] D.J. Blubaugh and G.M. Cheniae, in: N. Murata (Ed.), *Research in Photosynthesis*, Vol. II, Kluwer Academic Publishers, 1992, pp. 361–364.
- [44] D.J. Blubaugh, G.M. Cheniae, *Biochemistry* 29 (1990) 5109–5118.
- [45] M. Ebina and T. Yamashita, in: N. Murata (Ed.), *Research in Photosynthesis*, Vol. II, Kluwer Academic Publishers, 1992, pp. 389–392.
- [46] M. Qian, S.F. Al-Khalidi, C. Putnam-Evans, T.M. Bricker, R.L. Burnap, *Biochemistry* 36 (1997) 15244–15252.
- [47] T.-A. Ono, Y. Inoue, *Biochim. Biophys. Acta* 723 (1983) 191–201.
- [48] S.D. Betts, J.R. Ross, E. Pichersky, C.F. Yocum, *Biochemistry* 35 (1996) 6302–6307.
- [49] H.M. Gleiter, E. Haag, J.-R. Shen, J.J. Eaton-Rye, A.G. Seeliger, Y. Inoue, W.F.J. Vermaas, G. Renger, *Biochemistry* 34 (1995) 6847–6856.
- [50] R. Debus, in: H. Sigel (Ed.), *Metal Ions in Biological Systems*, Vol. 37, Marcel Dekker, 2000, pp. 657–710.
- [51] C. Büchel, J. Barber, G.M. Ananyev, S. Eshaghi, R. Watt, G.C. Dismukes, *Proc. Natl. Acad. Sci. USA* 96 (1999) 14288–14293.
- [52] A. Seidler, *Biochim. Biophys. Acta* 1277 (1996) 35–60.
- [53] A. Seidler, A.W. Rutherford, *Biochemistry* 35 (1996) 12104–12110.
- [54] R.L. Burnap, M. Qian, C. Pierce, *Biochemistry* 35 (1996) 874–882.
- [55] M. Rova, F. Mamedov, A. Magnuson, P.-O. Fredricksson, S. Styring, *Biochemistry* 37 (1998) 11039–11045.
- [56] A. Magnuson, M. Rova, F. Mamedov, P.-O. Fredricksson, S. Styring, *Biochim. Biophys. Acta* 141 (1999) 180–191.
- [57] G.M. Ananyev, L. Zaltsman, R.A. McInturff and G.C. Dismukes, in: G. Garob (Ed.), *Photosynthesis: Mechanisms and Effects (Proceedings XIth International Photosynthesis Congress)*, Kluwer, Dordrecht, 1998, pp. 1347–1350.
- [58] G.M. Ananyev, A. Murphy, Y. Abe, G.C. Dismukes, *Biochemistry* 38 (1999) 7200–7209.
- [59] W. Ruttlinger, G.C. Dismukes, *Chem. Rev.* 97 (1997) 1–24.
- [60] M.L. Ghirardi, T.W. Lutton, M. Seibert, *Biochemistry* 35 (1996) 1820–1828.
- [61] S. Izawa, D. Ort, *Biochim. Biophys. Acta* 357 (1974) 127–143.
- [62] M. Osawa, M.B. Swindells et al., *J. Mol. Biol.* 276 (1998) 165–176.
- [63] C.J. Lockett, C. Demerou, S.J. Bowden, J.H.A. Nugent, *Biochim. Biophys. Acta* 1016 (1990) 213–218.
- [64] G.M. Ananyev, G.C. Dismukes, *Biochemistry* 36 (1997) 11342–11350.
- [65] K.A. Campbell, D.A. Force, P.J. Nixon, F. Dole, B.A. Diner, R.D. Britt, *J. Am. Chem. Soc.* 122 (2000) 3754–3761.
- [66] G.M. Ananyev, G.C. Dismukes, *Biochemistry* 35 (1996) 14608–14617.
- [67] D.F. Ghanotakis, G.T. Babcock, C.F. Yocum, *FEBS Lett.* 167 (1986) 127–130.
- [68] T.-A. Ono, Y. Inoue, *Arch. Biochem. Biophys.* 275 (1989) 440–448.
- [69] M. Sivaraja, J. Tso, G.C. Dismukes, *Biochemistry* 28 (1989) 9459–9464.
- [70] A. Boussac, J.-L. Zimmerman, A.W. Rutherford, *Biochemistry* 28 (1989) 8989–8994.
- [71] R.M. Cinco, J.H. Robblee, A. Rompel, C. Fernandez, V.K. Yachandra, K. Sauer, M.P. Klein, *J. Phys. Chem. B* 102 (1998) 8248–8256.
- [72] T.-A. Ono and Y. Inoue, in: M. Baltischeckfsky (Ed.), *Current Research in Photosynthesis*, Vol. I, Kluwer Academic Press, Dordrecht, 1990, pp. 701–708.
- [73] J. Tso, M. Sivaraja, C.D. Dismukes, *Biochemistry* 30 (1991) 4734–4739.

- [74] G.C. Dismukes, *Chem. Scr.* 28a (1988) 99–104.
- [75] M. Qian, L. Dao, R.J. Debus, R.L. Burnap, *Biochemistry* 38 (1999) 6070–6081.
- [76] C. Chen, J. Kazimir, G.M. Cheniae, *Biochemistry* 34 (1995) 13511–13526.
- [77] P.J. Booth, A.W. Rutherford, A. Boussac, *Biochim. Biophys. Acta* 1277 (1996) 127–134.
- [78] T.-A. Ono, H. Mino, *Biochemistry* 38 (1999) 8778–8785.
- [79] A.C. Kulikov, V.R. Bogatyrenko, G.I. Likhtenstein, S.I. Allakherdiev, V.V. Klimov, V.A. Shuvalov, A.A. Krasnovsky, *Biofizika* 28 (1983) 357–363.
- [80] A. Boussac, A.W. Rutherford, *Biochemistry* 27 (1988) 3476–3483.
- [81] D.T. Richens, *Chemistry of Aqua Ions*, J. Wiley, Chichester, 1997.
- [82] J. Matysik, Alia, G. Nachtegaal, H.J. van Gorkom, A.J. Hoff, H.J.M. de Groot, *Biochemistry* 39 (2000) 6751–6755.
- [83] M. Zheng, G.C. Dismukes, *Inorg. Chem.* 35 (1996) 3307–3319.
- [84] G.C. Dismukes, W. Ruettinger, A.E.M. Boelrijk and D. Ho, in: G. Garob (Ed.), *Proceedings XIth International Photosynthesis Congress*, Vol. II, Kluwer Academic Publishers, 1998, pp. 1259–1264.
- [85] C. Preston, R. Pace, *Biochim. Biophys. Acta* 810 (1985) 388–391.
- [86] H. Wincencjusz, H.J. van Gorkom, C.F. Yocum, *Biochemistry* 36 (1997) 3663–3670.
- [87] H. Wincencjusz, C.F. Yocum, H.J. van Gorkom, *Biochemistry* 37 (1998) 8595–8604.
- [88] T.-A. Ono, J.-L. Zimmerman, Y. Inoue, A.W. Rutherford, *Biochim. Biophys. Acta* 851 (1986) 193–201.
- [89] M. Baumgarten, J.S. Philo, G.C. Dismukes, *Biochemistry* 29 (1990) 10814–10822.
- [90] D.A. Force, D.W. Randall, R.D. Britt, *Biochemistry* 36 (1997) 12062–12070.
- [91] J.M. Bove, F.R. Whatley, D.I. Arnon, *Z. Nat.forsch.* 18b (1963) 683–688.
- [92] C.F. Yocum, *Biochim. Biophys. Acta* 1059 (1991) 1–15.
- [93] G.C. Dismukes, M. Zheng, R. Hutchins, J.S. Philo, *Biochem. Soc. Trans.* 22 (1994) 323–327.
- [94] P. Mathur, M. Crowder, G.C. Dismukes, *J. Am. Chem. Soc.* 109 (1987) 5227–5232.
- [95] X.S. Tang, B.A. Diner, A.S. Larsen, M.L. Gilchrist, G.A. Lorigan, R.D. Britt, *Proc. Natl. Acad. Sci. USA* 91 (1994) 704–708.
- [96] V.J. DeRose, V.K. Yachandra, A.E. McDermott, R.D. Britt, K. Sauer, M.P. Klein, *Biochemistry* 30 (1991) 1335–1341.
- [97] H.A. Chu, A.P. Nguyen, R.J. Debus, *Biochemistry* 34 (1995) 5859–5882.
- [98] V.K. Yachandra, K. Sauer, M.P. Klein, *Chem. Rev.* 96 (1996) 2927–2950.
- [99] W. Liang, T.A. Roelofs, R.M. Cinco, A. Rompel, M.J. Latimer, W.O. Yu, K. Sauer, M.P. Klein, Y.K. Yachandra, *J. Am. Chem. Soc.* 122 (2000) 3399–3412.
- [100] R. Manchandra, G.W. Brudvig, R.H. Crabtree, *Coord. Chem. Rev.* 144 (1995) 1–38.
- [101] N.A. Law, J.W. Kampf, V.L. Pecoraro, *Inorg. Chim. Acta* 297 (2000) 252–254.
- [102] K. Hasegawa, T.-A. Ono, Y. Inoue, M. Kusunoki, *Bull. Chem. Soc. Jpn.* 72 (2000) 1013–1023.
- [103] S. Wang, M.S. Wemple, J. Yoo, K. Folting, J.C. Huffman, K.S. Hagen, D.N. Hendrickson, G. Christou, *Inorg. Chem.* 39 (2000) 1501–1513.
- [104] W. Hillier, J. Messinger, T. Wydrzynski, *Biochemistry* 37 (1998) 16908–16914.
- [105] W. Hillier, T. Wydrzynski, *Biochemistry* 39 (2000) 4399–4405.
- [106] J. Messinger, M. Badger, T. Wydrzynski, *Proc. Natl. Acad. Sci. USA* 92 (1995) 3209–3213.
- [107] B. Forbush, B. Kok, M.P. McGloin, *Photochem. Photobiol.* 11 (1971) 457–475.
- [108] J. Mano, M.-A. Takahashi, K. Asada, *Biochemistry* 26 (1987) 2495–2501.
- [109] D.L. Fine, W.D. Frasch, *Biochemistry* 31 (1992) 12204–12210.
- [110] G.M. Ananyev, T. Wydrzynski, G. Renger, V.V. Klimov, *Biochim. Biophys. Acta* 1100 (1992) 303–311.
- [111] V.V. Klimov, G.M. Ananyev and O.M. Zastryzhnaya, in: N. Murata (Ed.), *Research in Photosynthesis*, Vol. II, Kluwer Academic Publishers, 1992, pp. 441–444.
- [112] T. Wydrzynski, I. Angstrom, T. Vannagard, *Biochim. Biophys. Acta* 973 (1989) 23–28.
- [113] J. Mano, K. Kawamoto, G.C. Dismukes, K. Asada, *Photosynth. Res.* 38 (1993) 433–440.
- [114] G.C. Dismukes, *Chem. Rev.* 96 (1996) 2909–2926.